Influence of A-site disorder on the half-doped manganites

Jiyu Fan, Langsheng Ling, Li Pi, Yang Wang, Yue Ying et al.

Additional information on J. Appl. Phys.
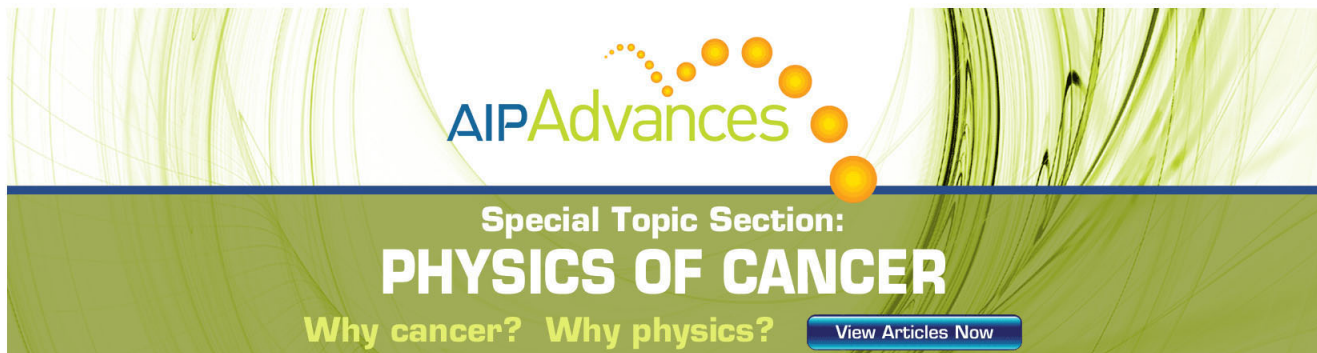
Influence of *A*-site disorder on the half-doped manganites

Jiyu Fan,[a)] Langsheng Ling, Li Pi, Yang Wang, Yue Ying, and Yuheng Zhang
*Hefei High Magnetic Field Laboratory, University of Science and Technology of China, Hefei 230026,
People's Republic of China*

The electronic transport and magnetism in half-doped $Nd_{0.50}Ca_{0.25}Sr_{0.25}MnO_3$ manganites have been investigated. Contrary to general half-doped system, it only displays a paramagnetic-ferromagnetic phase transition associated with an insulator-metal transition instead of with any features of charge ordering. With the decrease of temperature, an electronic phase separation and spin glass state occur in low temperature. We suggest that the *A*-site cation disorder induced by the size mismatch between Sr^{2+} ion and Ca^{2+} ion is mainly responsible for this phenomenon. © *2006 American Institute of Physics*. [DOI: 10.1063/1.2338136]

I. INTRODUCTION

The physics of manganite perovskites has been studied extensively in the last decade following the discovery of colossal magnetoresistance in the hole-doped $R_{1-x}A_xMnO_3$ (*R* =trivalent rare earth and *R*=divalent alkaline earth).[1,2] These materials show an unprecedented coupling between spin, charge, orbital, and lattice degree of freedom.[3–5] Meanwhile, it is widely accepted that the *A*-site average ionic radius $\langle r_A \rangle$ is a key parameter to determine what phase is realized in $R_{1-x}A_xMnO_3$.[6,7] For large $\langle r_A \rangle$ compounds with hole-doping concentration of $0.17 \leq x \leq 0.4$, the ground state usually appears to be a ferromagnetic (FM) metallic state, which can be explained in terms of the double exchange mechanism associated with Jahn-Teller effect.[8–11] In perovskite manganites, the effective one-electron bandwidth of e_g band, which is mainly responsible for the systematic magnetic state and the electronic transport, is intensively dependent on the MnO_6 octahedra distortion.[12] When the *A*-site average radius decreases, the tilting of the MnO_6 octahedra in the perovskites structure increases and hence the effective one-electron bandwidth becomes narrow and the double exchange mechanism is suppressed. As a result, the FM metallic state is replaced by the other phase, e.g., orbital ordering state, charge ordering state, and antiferromagnetic (AFM) insulator.[13,14] The in-depth investigations show that the effect of *A*-site average ionic radius is more profound on the charge ordering (CO) in the half-doped manganites. Arulraj *et al.* verified that the CO phase existed only in the average radius $\langle r_A \rangle$ varing over the range of 1.24–1.13 Å.[15] Sundaresan *et al.* found that the CO state was suppressed remarkably by the La/Y ionic substitution in $Pr_{1-x}Ca_xMnO_3$.[16] Additionally, the property that the stability of CO state in a magnetic field is sensitive to *A*-site average radius was observed by Tokura and Nagaosa.[5]

Note that the *A*-site averaged radius is an essential ingredient to CO system, the investigation on the change of $\langle r_A \rangle$ should be valuable. In half-doped manganites, we find that the $Nd_{0.5}Ca_{0.5}MnO_3$ and $Nd_{0.5}Sr_{0.5}MnO_3$ are two different CO materials. $Nd_{0.5}Ca_{0.5}MnO_3$ initially forms CO phase at

$T_{CO}=250$ K and then undergoes a transition from PM to CE-type AFM state around 160 K.[17] On the contrary, $Nd_{0.5}Sr_{0.5}MnO_3$ firstly experiences a PM-FM transition at 250 K and then enters into CO/AFM phase at 150 K.[18] Moreover, the recent experimental evidences also show that its ground state consists of not only FM and CE-type AFM phase but also *A*-type AFM phase.[19] Additionally, at the earlier stage, Rao *et al.* have provided a clear phase graph about the CO transition temperature versus *A*-site average radius through a thoughtful investigation of the effect of the size of the *A*-site cations on the CO state in $Nd_{0.5}Ca_{0.5-x}Sr_xMnO_3$ as *x* changes from 0 to 0.5 but without $x=0.25$.[20,21] Here, we suppose that if we make use of Sr^{2+} ion in quantity of 25% to substitute Ca^{2+} ion in $Nd_{0.5}Ca_{0.5}MnO_3$, what changes will happen to the CO phase in the $Nd_{0.5}Ca_{0.25}Sr_{0.25}MnO_3$ material? Unexpectedly, we have not observed any CO characteristic as shown in the pristine $Nd_{0.5}Ca_{0.5}MnO_3$/ $Nd_{0.5}Sr_{0.5}MnO_3$. Instead, it only exhibits a typical PM-FM phase transition associated with an insulator-metal transition, similar to the universal finding in $R_{0.7}A_{0.3}MnO_3$ system.[22,23] Meanwhile, an electronic phase separation of FM and AFM was observed in broad temperature range. At low temperature, a spin glass feature occurs. We suggest that the *A*-site cation disorder induced by the size mismatch between Sr^{2+} ion and Ca^{2+} ion is mainly responsible for this phenomenon. Due to the emergence of disorder, the pristine homogeneous strain field was destroyed into inhomogeneous one, which directly destabilizes long-range CO phase and thus results in an absence of CO phase in $Nd_{0.5}Ca_{0.25}Sr_{0.25}MnO_3$ system even if it retains a commensurate stoichiometric ratio of $Mn^{3+}:Mn^{4+}=1$

II. EXPERIMENTAL DETAILS

Polycrystalline sample $Nd_{0.5}Ca_{0.25}Sr_{0.25}MnO_3$ was synthesized by the conventional solid-state reaction method with high pure Nd_2O_3, $SrCO_3$, $CaCO_3$, and MnO_2. (For comparison, $Nd_{0.5}Ca_{0.5}MnO_3$ and $Nd_{0.5}Sr_{0.5}MnO_3$ were prepared with the same method.) The mixture was preheated in air at 900 °C for 24 h. Afterwards the powder was ground and heated at 1200 °C for 30 h. Finally, it was reground, palletized, and sintered for another 40 h at 1350 °C, and then

---

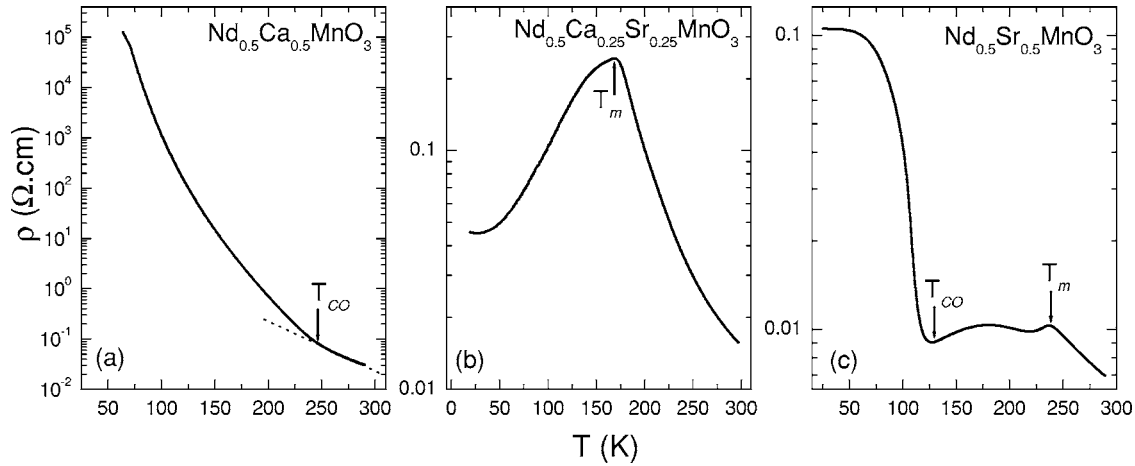[a)]Electronic mail: jiyufan@ustc.edu

FIG. 1. Temperature dependence of resistivity for $Nd_{0.50}Ca_{0.50}MnO_3$ (a), $Nd_{0.50}Ca_{0.25}Sr_{0.25}MnO_3$ (b), and $Nd_{0.50}Sr_{0.50}MnO_3$ (c); T_{CO} (temperature of charger ordering); T_m (temperature of insulator-metal transition).

cooled down to room temperature in the furnace. Powder x-ray diffraction was employed on Japan Rigaku D/max -$\gamma\alpha$ rotating powder diffractometer using Cu $K\alpha$ radiation to check the structure and phase purity. All the samples were proved to be single-phase orthorhombic structure. The resistivity (ρ) was measured by standard four-probe method. The magnetization (M) measurement was performed using the Quantum Design superconducting quantum interferece device under 0.01 T magnetic field in the range of 5–300 K. The $M(H)$ curve was measured with sweep field from −6 to 6 T. The electron-spin-resonance (ESR) spectra were obtained from JES-FA200 spectrometer at 9.06 GHz. Raman scattering spectrum was obtained on a confocal laser micro-Raman spectrometer with laser of the wavelength of 514.5 nm.

III. RESULTS AND DISCUSSION

The temperature dependence of resistivity $\rho(T)$ curves for three samples is shown in Fig. 1. In the case of $Nd_{0.5}Ca_{0.5}MnO_3$, it displays an insulating behavior at whole measured temperature range except for a small kink around 250 K, which is an indication of CO phase. In contrast, in

Fig. 1(c), the compound $Nd_{0.5}Sr_{0.5}MnO_3$ initially undergoes an insulator-metal transition near 240 K (marked with T_m) and then a steep increase of resistivity occurs in 130 K, exhibiting a CO phase transition. Obviously, both $Nd_{0.5}Ca_{0.5}MnO_3$ and $Nd_{0.5}Sr_{0.5}MnO_3$ compounds are typical CO systems even their CO temperatures T_{CO} are different. For $Nd_{0.5}Ca_{0.25}Sr_{0.25}MnO_3$ sample, it seems to belong to CO family judging from the nominal stoichiometric composition because its A-site average radius was adjusted slightly, ($Nd_{0.5}Ca_{0.5}MnO_3$: $\langle r_A\rangle$=1.19 Å; $Nd_{0.5}Ca_{0.25}Sr_{0.25}MnO_3$: $\langle r_A\rangle$ =1.21 Å) and these two end compounds are CO materials as well. However, on the contrary to our assumptions, the conductivity of $Nd_{0.5}Ca_{0.25}Sr_{0.25}MnO_3$ displays a common insulator-metal transition at T_m=175 K, without any evidences of CO phase. This property seems to be apt to that reported extensively in optimal doped system $R_{0.7}A_{0.3}MnO_3$ with carrier concentration x=0.3.[22,23] In fact, the Sr^{2+} substitution for Ca^{2+} does not change the commensurate ratio of Mn^{3+}:Mn^{4+}=1, which is a vantage condition for CO formation in narrow-band manganites. This different transport properties reflect a marked change in the magnetic behavior.

The magnetization was measured with zero-field-cooling (ZFC) mode (marked with solid circle) and field-cooling
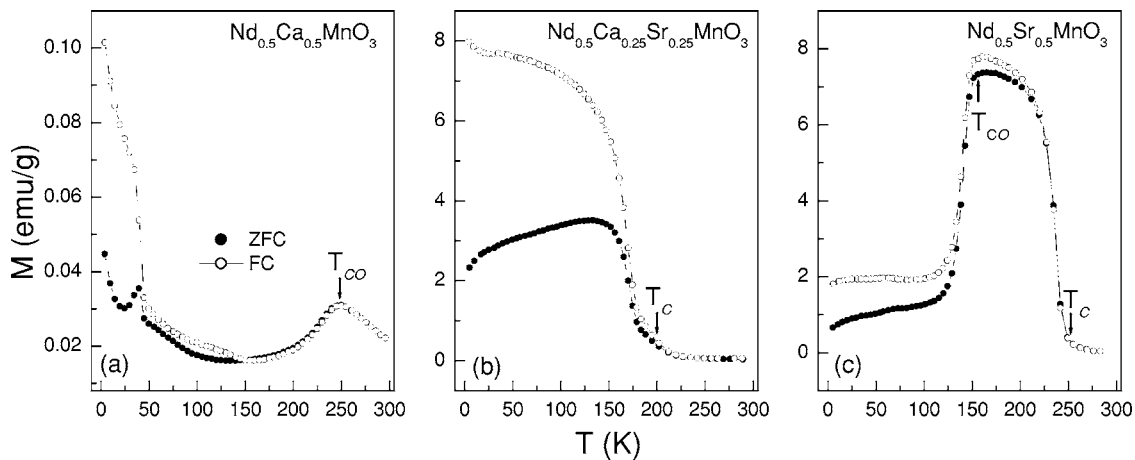

FIG. 2. Temperature dependence of the magnetization for $Nd_{0.50}Ca_{0.50}MnO_3$ (a), $Nd_{0.50}Ca_{0.25}Sr_{0.25}MnO_3$ (b), and $Nd_{0.50}Sr_{0.50}MnO_3$ (c); T_{CO} (temperature of charger ordering); T_C (Curie temperature).
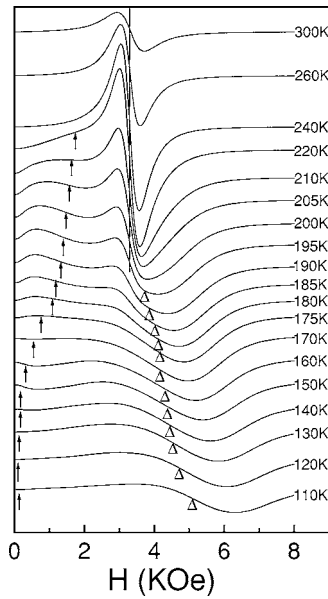
FIG. 3. Electronic spin resonance spectra of $Nd_{0.50}Ca_{0.25}Sr_{0.25}MnO_3$ at different temperatures; PM, FM, and AFM peaks are marked with straight line, ↑, and △, respectively.

(FC) mode (marked with open circle) for these three samples in the temperature range of 5–300 K. As shown in Fig. 2(a), a little peak occurs in ZFC $M(T)$ curve around 250 K, which just corresponds to the kink in the $\rho(T)$ curve of $Nd_{0.5}Ca_{0.5}MnO_3$ sample. This is a signal of the formation of CO phase. As the decrease of temperature, there happens AFM transition at 150 K. For $Nd_{0.5}Sr_{0.5}MnO_3$ sample, it firstly undergoes PM-FM phase transition nearly T_C ~250 K [the Curie temperature T_C is defined as the inflection point of ZFC $M(T)$ curve] and then enters into CO phase around 150 K demonstrated by the abrupt decrease in magnetization. Similarly, the evolution of its magnetism corresponds to the change of its $\rho(T)$ curves as well. These behaviors are completely the same to the observation by Millange *et al.*[17] and Kajimoto *et al.*[18] For $Nd_{0.5}Ca_{0.25}Sr_{0.25}MnO_3$ compound, it only exhibits a PM-FM transition. The Curie temperature T_C is 195 K. At $T \leqslant 125$ K, the slight decrease in magnetization implies the emergence of weak AFM coupling. Additionally, the FC

curve does not coincide with ZFC curves below T_C. This large separation is a characteristic of spin glass state. Generally, spin glass state stems from a strong competition between opposite interactions, e.g., FM coupling and AFM coupling. That is to say, the presence of spin glass means that this system is inhomogeneous and does not possess long-range ordering structure. Experimentally, the evidences of systematic inhomogeneity have been verified not only in B-sites doped manganites but also in the spinel structure $FeCr_{2-x}Al_xS_4$.[24,25] Moreover, the existence of inhomogeneity sometimes causes an electronic phase separation. To clarify this point in $Nd_{0.5}Ca_{0.25}Sr_{0.25}MnO_3$, we performed ESR spectra measurement at different temperatures, which is a powerful microscopic probe to reveal magnetic phase transition and magnetic ordering.

As shown in Fig. 3, in the high temperature above T_C, a clear PM resonance peak occurs in the position of $H = 3200$ Oe (marked with straight line). Below T_C, it splits into two resonance peaks, one shifting to low field region (marked with ↑) while another shifting to high field region (marked with △). The former is referred to FM resonance peak, which has been extensively observed in $La_{1-x}A_xMnO_3$,[26] whereas the latter is attributed to AFM resonance peak as shown in $LaMn_{1-x}Cr_xO_3$.[27] In fact, here, the FM peak has occurred early in $T = 240$ K. The emergence of FM resonance peak before PM-FM transition implies a fact that nanometer FM clusters have imbedded in PM matrix. Such a behavior was also observed in $La_{0.7}Ca_{0.3}MnO_3$ by De Teresa *et al.*[28] and in A-site disorder $Pr_{0.6}R_{0.1}Sr_{0.3}MnO_3$ by Rama *et al.*[29] With the further decrease of temperature, the FM and AFM resonance peaks continuously shift to low field region and high field region, respectively. Therefore, the coexistence of FM and AFM phases remains in a broad temperature region of 195–110 K, displaying an electronic phase separation.

The coexistence of FM phase and AFM phase can be also verified from the field dependent magnetization $M(H)$ curves in Fig. 4. Clearly, at all measured temperature points, the robust magnetization reflects a typical feature of ferromagnetism, while a slight hysteresis loop at 150 K and an obvious one at 100 K display a behavior of antiferromagnetism. Although the hysteresis loop was not observed at
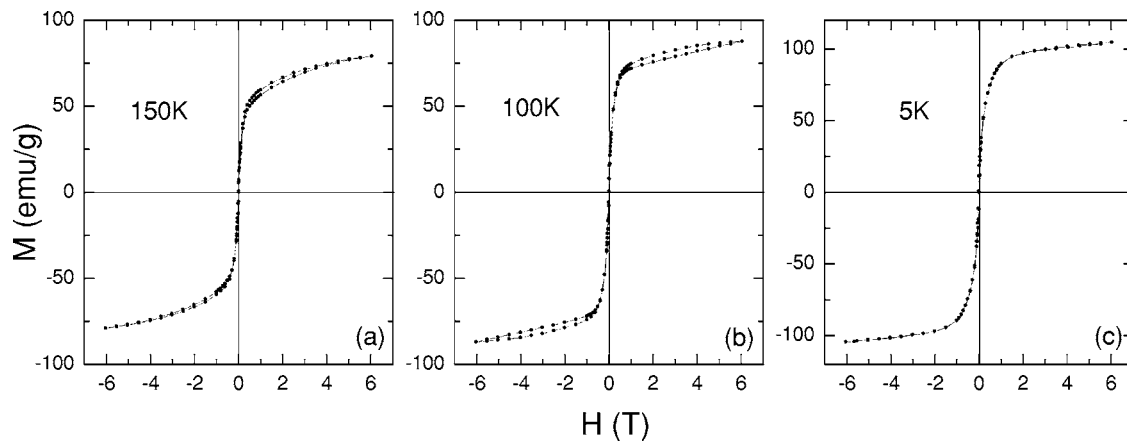

FIG. 4. The $M(H)$ curve for $Nd_{0.50}Ca_{0.25}Sr_{0.25}MnO_3$ at 150, 100, and 5 K.

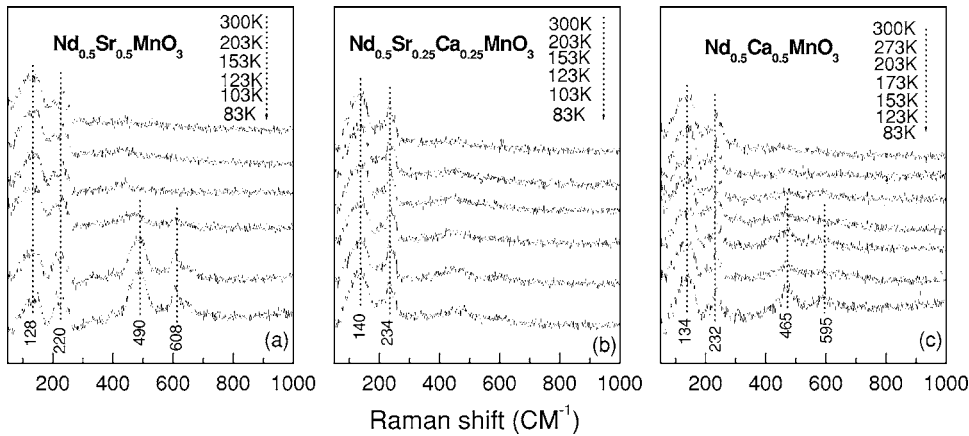FIG. 5. Temperature dependence of Raman spectra for $Nd_{0.50}Ca_{0.50}MnO_3$, $Nd_{0.50}Ca_{0.25}Sr_{0.25}MnO_3$, $Nd_{0.50}Sr_{0.50}MnO_3$.

5 K, it might be due to the progressing inner FM coupling and external field forcing it to melt into FM matrix. In fact, we do not find any abnormal properties except for a slight upturn at lowest temperature from $\rho(T)$ curve and a smaller decrease in magnetization blow 125 K from ZFC $M(T)$ curve, suggesting that the AFM coupling only occurs in a smaller extent.

Raman spectroscopy is an efficient tool for the study of local electronic, lattice, and spin degree of freedom as well as coupling between them. For one CO system, the carriers will become strongly localized once the temperature decreases below T_{CO}. And then, a strong electron-phonon interaction will occur. Therefore, the temperature dependence of Raman spectroscopy is carried out for the three samples discussed above. As shown in Fig. 5, all samples display a similar low-energy vibration modes. Furthermore, with decreasing temperature, these modes do not exhibit a noticeable change. However, for $Nd_{0.5}Sr_{0.5}MnO_3$ and $Nd_{0.5}Ca_{0.5}MnO_3$ samples, two additional vibration modes occur in the site of 490/608 and 465/596 cm^{-1}, which are associated with Jahn-Teller distortion and bending of MnO_6 octahedra, respectively. These behaviors are very similar to the observation in the polycrystalline $La_{0.5}Ca_{0.5}MnO_3$ and the single crystal $Nd_{0.5}Sr_{0.5}MnO_3$.[30,31] Generally, Raman spectra change dramatically as the temperature decreases below T_{CO}. As we know, Raman spectra are determined by two contributions: the light interaction with phonons and the light interaction with free charge carriers. When the $Nd_{0.5}Sr_{0.5}MnO_3$ and $Nd_{0.5}Ca_{0.5}MnO_3$ systems undergo a CO transition, the carriers are strongly localized and the static Jahn-Teller distortion grows into a prominent one. Thus, the diminishment of carrier screening effect due to carrier localization and the enhancement of distortion for MnO_6 octahedra will induce some new Raman modes to appear. In fact, the two Raman modes have been recognized to be a signature of CO formation by Granado *et al.*[30] and Choi *et al.*[31] In contrast, as one system enters into FM metal region, such as in the current $Nd_{0.5}Ca_{0.25}Sr_{0.25}MnO_3$ compound, the delocalized carriers cause a rise of carriers scattering and a reduction of carriers screening effect. Moreover, the previous static Jahn-Teller distortion is suppressed simultaneously and transforms into dynamic one. As a result, the intensity of the two Raman vibration modes is weakened so that it is usually difficult to observe them.

Based on the results above, the absence of CO phase in $Nd_{0.5}Ca_{0.25}Sr_{0.25}MnO_3$ can be understood from the following scenario. Due to the large mismatch in ionic size between Ca^{2+} and Sr^{2+} ($r_{Ca}=1.18$ Å and $r_{Sr}=1.31$ Å), the Sr^{2+} ionic substitution for Ca^{2+} induces a considerable disorder on A site. Accordingly, the previous homogeneous strain field is broken into some inhomogeneous ones. Under this situation, it becomes very difficult for the formation of long-rang CO phase. In theory, Mathur and Littlewood[32] and Caldervoón *et al.*[33] had testified that the long-range strain is very important in CO manganites. Recently, Ahn *et al.* further elucidated that the uniform strain plays a key role in stabilizing the orbital/charge ordering pattern in the half-doped manganites.[34] In other words, the inhomogeneous strain will destabilize orbital/charge ordering phase. Therefore, the A-site cation disorder is mainly responsible for the absence of CO phase in $Nd_{0.5}Ca_{0.25}Sr_{0.25}MnO_3$. Similar to the present observation in bulk samples, the role of strain which destabilizes CO phase was also found in the half-doped manganite thin films.[35] Prellier *et al.* did not find CO phase in the $Nd_{0.5}Sr_{0.5}MnO_3$ thin film because the epitaxial strain due to the lattice mismatch between the substrate and the film prevented it from producing structural change at $T < T_{CO}$ as in bulk and single crystal.[36] Chen *et al.* also proposed that the epitaxial strain could influence insulator-metal transition in the thin film samples.[37–39] Therefore, both the interior strain and exterior strain play a key role in stabilizing the CO phase. In addition, due to the appearance of disorder, Sr^{2+} ions might congregate some regions while Ca^{2+} ions might accumulate in other ones. In the Sr^{2+} rich region, it prefers to be the FM coupling, but in the Ca^{2+} rich region, it tends to be AFM coupling. Consequently, the coexistence and competition between FM and AFM phases result in the appearance of electronic phase separation and spin glass in low temperature.

IV. CONCLUSION

In summary, the transport and magnetic properties of $Nd_{0.50}Ca_{0.25}Sr_{0.25}MnO_3$ have been studied. With the decrease of temperature, it experiences a PM-FM phase transition associated with an insulator-metal transition but without an appearance of charge ordering. Meanwhile, an electronic phase separation and spin glass state occur in low temperature. We

suggest that the *A*-site cation disorder induced by the size mismatch between Sr^{2+} ion and Ca^{2+} ion is mainly responsible for it. Due to the appearance of disorder, the inhomogeneous strain will destabilize orbital/charge ordering phase, which results in an absence of charge ordering state in half-doped $Nd_{0.50}Ca_{0.25}Sr_{0.25}MnO_3$ system.

ACKNOWLEDGMENTS

[1] R. von Helmolt, J. Wecker, B. Holzapfel, L. Schultz, and K. Samwer, Phys. Rev. Lett. **71**, 2331 (1993).

[2] S. Jin, T. H. Tiefel, M. McCormack, R. A. Fastnacht, R. Ramesh, and L. H. Chen, Science **264**, 413 (1994).

[3] S. Mori, C. H. Chen, and S.-W. Cheong, Phys. Rev. Lett. **81**, 3972 (1998).

[4] C. N. R. Rao and A. K. Cheetham, Science **276**, 911 (1999).

[5] Y. Tokura and N. Nagaosa, Science **288**, 462 (2000).

[6] L. M. Rodriguez-Martinez and J. P. Attfield, Phys. Rev. B **54**, R15622 (1996).

[7] B. Raveau, A. Maignan, C. Martin, and M. Hervieu, Chem. Mater. **10**, 2641 (1998).

[8] A. Asamistu, Y. Moritomo, Y. Tomika, T. Arima, and Y. Tokura, Nature (London) **373**, 407 (1995).

[9] C. Zener, Phys. Rev. **82**, 403 (1951).

[10] A. J. Millis, P. B. Littlewood, and B. J. Shraiman, Phys. Rev. Lett. **74**, 5144 (1995).

[11] J. S. Zhou and J. B. Goodenough, Phys. Rev. Lett. **80**, 2665 (1998).

[12] J. Töpfer and J. B. Goodenough, Chem. Mater. **9**, 1467 (1997).

[13] H. Y. Hwang, S.-W. Cheong, P. G. Radaelli, M. Marezio, and B. Batlogg, Phys. Rev. Lett. **75**, 914 (1995).

[14] Z. Jirak, S. Krupicka, Z. Simsa, M. Dlouha, and Z. Vratislav, J. Magn. Magn. Mater. **53**, 153 (1985).

[15] A. Arulraj, P. N. Santhosh, R. Srinivasa Gopalan, A. Guha, A. K. Raychaudhuri, and C. N. R. Rao, J. Phys.: Condens. Matter **10**, 8497 (1998).

[16] A. Sundaresan, A. Maignan, and B. Raveau, Phys. Rev. B **56**, 5092 (1997).

[17] F. Millange, S. de Brion, and G. Chouteau, Phys. Rev. B **62**, 5619 (2000).

[18] R. Kajimoto, H. Yoshizawa, H. Kawano, H. Kuwahara, Y. Tokura, K. Ohoyama, and M. Ohashi, Phys. Rev. B **60**, 9506 (1999).

[19] H. Kawano-Furukawa, R. Kajimoto, H. Yoshizawa, Y. Tomioka, H. Kuwahara, and Y. Tokura, Phys. Rev. B **68**, 174422 (2003).

[20] C. N. R. Rao, P. N. Santhosh, R. S. Singh, and A. Arulraj, J. Solid State Chem. **135**, 169 (1998).

[21] C. N. R. Rao, A. Arulraj, P. N. Santosh, and A. K. Cheetham, Chem. Mater. **10**, 2714 (1998).

[22] K. Chahara, T. Ohno, M. Kasai, and Y. Kosono, Appl. Phys. Lett. **63**, 1990 (1994).

[23] A. Urushibara, Y. Moritomo, T. Tomioka, A. Asamitsu, G. Kido, and Y. Tokura, Phys. Rev. B **51**, 14103 (1995).

[24] K. Ghosh, S. B. Ogale, R. Ramesh, R. L. Greene, T. Venkatesan, K. M. Gapchup, Ravi Bathe, and S. I. Paitil, Phys. Rev. B **59**, 533 (1999).

[25] Z. R. Yang, S. Tan, and Y. H. Zhang, Appl. Phys. Lett. **79**, 3645 (2001).

[26] S. B. Oseroff, M. Torikachvili, J. Singley, S. Ali, S.-W. Cheong, and S. Schultz, Phys. Rev. B **53**, 6521 (1996).

[27] Y. Sun, W. Tong, X. Xu, and Y. Zhang, Phys. Rev. B **63**, 174438 (2001).

[28] J. M. De Teresa *et al.*, Nature (London) **386**, 256 (1997).

[29] N. Rama, M. S. Ramachandra Rao, V. Sankaranarayanan, P. Majewski, S. Gepraegs, M. Ople, and R. Gross, Phys. Rev. B **70**, 224424 (2004).

[30] E. Granado *et al.*, Phys. Rev. B **58**, 11435 (1998).

[31] K.-Y. Choi *et al.*, J. Phys.: Condens. Matter **15**, 3333 (2003).

[32] N. D. Mathur and P. B. Littlewood, Solid State Commun. **119**, 271 (2001).

[33] M. J. Calderón, A. J. Millis, and K. H. Ahn, Phys. Rev. B **68**, 100401 (2003).

[34] K. H. Ahn, T. Lookman, and A. R. Bishop, Nature (London) **428**, 401 (2004).

[35] P. Wagner, I. Gordon, A. Vantomme, D. Dierickx, M. J. Van Bael, V. V. Moshchalkov, and Y. Bruynseraede, Europhys. Lett. **41**, 49 (1998).

[36] W. Prellier, A. Biswas, M. Rajeswari, T. Venkatesan, and R. L. Greene, Appl. Phys. Lett. **75**, 397 (1999).

[37] X. J. Chen, S. Soltan, H. Zhang, and H.-U. Habermeier, Phys. Rev. B **65**, 174402 (2002).

[38] X. J. Chen, H.-U. Habermeier, and C. C. Almasan, Phys. Rev. B **68**, 132407 (2003).

[39] X. J. Chen, H.-U. Habermeier, H. Zhang, G. Gu, M. Varela, J. Santamaria, and C. C. Almasan, Phys. Rev. B **72**, 104403 (2005).